# An Atlas-based Variational Approach to Quantitative Susceptibility Mapping

Clare Poynton[1], Elfar Adalsteinsson[1,2], Edith V. Sullivan[3], Adolf Pfefferbaum[3], and William Wells III[1,4]

[1]*Health Sciences and Technology, Harvard - MIT, Cambridge, MA, United States,* [2]*Department of Electrical Engineering and Computer Science, MIT, Cambridge, MA, United States,* [3]*Department of Psychiatry & Behavioral Sciences, Stanford University School of Medicine, Stanford, CA, United States,* [4]*Department of Radiology, Harvard Medical School, Brigham and Women's Hospital, Boston, MA, United States*

## Introduction

Excessive iron deposition in specific regions of the brain is associated with neurodegenerative disorders such as Alzheimer's and Parkinson's disease [1]. Iron deposition causes changes in tissue magnetic susceptibility, resulting in magnetic field perturbations that can be modeled as the convolution of a dipole-like kernel and the spatial susceptibility map. In the Fourier domain, zeros at the magic angle and limited observations make inversion of the field ill-posed. In addition, 'biasfields' from external sources (i.e., tissue/air boundaries, mis-set shims) confound iron-related phase effects. Previous work has shown that a wave equation relating the Laplacian of the field to the D'Alembertian of susceptibility can be derived from a spatial formulation of the forward model, providing biasfield elimination and accurate susceptibility estimates when solved with a variational approach [2]. In this work, we present an atlas-based susceptibility mapping (ASM) technique that is based on the Laplacian of the spatial field model and incorporates a tissue/air atlas to resolve ambiguity between internal and external susceptibility sources.

## Methods

Quantitative susceptibility mapping (QSM) is a challenging problem because operations on susceptibility, such as the kernel, $K$, or the D'Alembertian, $\square$, cause information loss due to derivatives in $\square$ or zeros in the kernel, requiring some form of regularization or prior information for a complete solution. Probabilistic atlases are frequently used to compensate for missing information in MR acquisitions: in [3] it was shown that use of a tissue/air susceptibility atlas improves forward field calculations. Although [2] showed good results for phantom data, the regularization term assumed very similar spatial frequency structure between the magnitude image and susceptibility distribution, which may not be true for in-vivo brain data. Recently, the technique in [4] has shown good correlations with postmortem iron values, but relies on multi-angle acquisitions. The method in [5] achieved strong correlation with postmortem iron by inverting the Fourier-based forward model and using L1-norm regularization. Our ASM method uses a variational approach as defined in Eq. 1. The Laplacian of the observed field, $B$, eliminates shims and low order biasfields that are a solution to the Laplace equation, and is proportional to the product of the main field strength, $B_0$, and the D'Alembertian of susceptibility, $\square\chi$. The weighting factor, $W$, is set to $|\Delta B|$, where $|\cdot|$ denotes the absolute value. Voxels in $W$ that fall within $2\sigma$ are set to 0, where $\sigma$ is the standard deviation of the signal in a noise region of the SWI magnitude image. To prevent the elimination of internal susceptibility distributions that are eigenfunctions of the forward model, the second term enforces agreement of the predicted and observed field in the brain via the binary mask $M_0$. An initial estimate of the biasfield due to external sources, $B_e$, is computed by convolving the Fourier-based kernel, $K_f$, with the estimate of external sources, $\chi_e^*$. External sources are modeled using the tissue/air atlas, $\chi_A$, and the Fourier-based forward model is inverted in Eq. 2, where $M$ is a mask derived from the magnitude image and enforces agreement where the signal is valid. In term 3, $M_0^C$, is a mask of the region outside the brain which enforces agreement with the estimate of external sources from Eq. 2 with strength depending on the weight $\lambda_3$. Eqs. 1 and 2 were solved using standard conjugate gradient techniques.

$$\arg\min_{\chi} \lambda_1 \left| W\left(\Delta B - \frac{B_0}{3}\square\chi\right)\right|_1 + \lambda_2 \left| M_0\left(B - \left(K_s\chi + B_e\right)\right)\right|_2^2 + \lambda_3 \left| M_0^C\chi\right|_2^2 \quad [1]$$

$$\chi_e^* = \arg\min_{\chi_e} \left| M\left(B - K_f\chi_e\right)\right|_2^2 \quad \text{where} \quad \chi_e^{(0)} = \chi_A \quad [2]$$

*Data Acquisition:* We obtained structural MRI and phase maps for 12 elderly subjects (mean= 74.4±7.6 years) and 11 younger adults (24±2.5 years) previously acquired by [6] on a 1.5 T GE Signa with 62 slices, 2.5mm thick: 3D SPGR for structural imaging, TR/TE=28/10ms, 256x256, 24cm; 3D SPGR with flow compensation for SWI and phase map reconstruction, TR/TE=58/40ms, 512x256, 24 cm. ROIs were automatically delineated on axial images as described in [6] and mean susceptibility estimates relative to $\chi_{water} \approx$ -9.1 ppm were computed in four brain regions: thalamus (TH), caudate (CD), putamen (PT) and globus pallidus (GP) and plotted against corresponding postmortem values from [7].

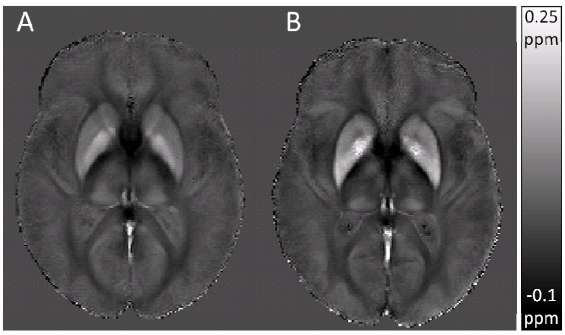


**Fig 1**. Group averages of ASM results for young (A) and elderly (B) subjects show an age dependent increase in estimated susceptibility values in sub-cortical regions known to accumulate iron in normal aging.

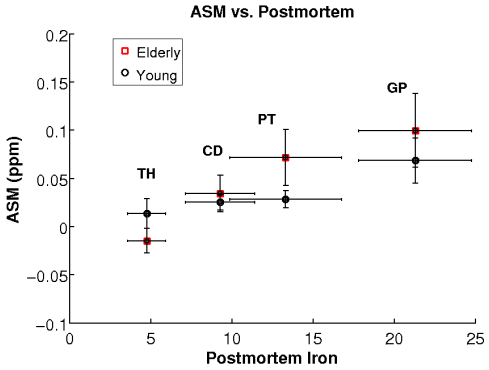


**Fig. 2**. Estimated relative susceptibility values show strong correspondence with postmortem iron concentrations (mg/100g) in young and elderly subjects.

## Results and Discussion

Fig 1. shows the average ASM results for young and elderly subjects, illustrating an age-dependent increase in iron concentration in sub-cortical structures. Mean susceptibility in both elderly and young subjects show strong correspondence with postmortem iron concentration (Fig 2), similar to that seen in [4], but does not require multiple acquisitions. In addition, ASM estimates show reduced variance in elderly and young subjects in TH, CD, and PT relative to results in [5], which may provide improved classification of patient populations in future clinical studies.

**References:** [1] Zecca L, et al. Nat Rev Neurosci, 2004, 5:863-73. [2] Poynton C, et al. ISMRM, 2011. [3] Poynton C, et al. MICCAI, 2009, 12(2):951-9. [4] Schweser et al. Neuroimage, 2011,54(4):2789-807 [5] Bilgic B, et al. Neuroimage, 2011. [6] Pfefferbaum et al. Neuroimage, 2009, 47(2):493-500 [7] Hallgren B, et al. J Neurochem, 1958,3(1):41-51.

**Acknowledgements: P41RR13218, AG017919, AA005965**